

Surface interactions and surface dynamics on a clean reconstructed W(100)

W. K. Han* and S.-C. Ying

Department of Physics, Brown University, Providence, Rhode Island 02912

(Received 20 September 1991)

We have extended our study of the surface dynamics of a clean W(100) to the region $T < T_c$. We have determined the surface phonon dispersion relations using a quasiharmonic approximation at low temperatures and a method of critical dynamics near T_c . We demonstrate here how the phonon band gap opens at the surface Brillouin-zone boundary, as the surface goes into the $c(2 \times 2)$ phase. We also show how the surface phonon excitation differs from the harmonic picture under the presence of strong anharmonic interactions and large critical fluctuations.

In the study of a surface structural phase transition, the understanding of surface dynamics is a challenging problem, besides that of static properties. It has been established experimentally^{1,2} and theoretically^{3,4} that the dynamics of a clean W(100) surface is very different from the simple harmonic picture in terms of the softening and damping of phonon excitations near its $c(2 \times 2)$ reconstruction.⁵ This is believed to be due to the anharmonic interactions and critical fluctuations. In our previous study⁶ of this surface, we have developed a model Hamiltonian that accounts very well for all of the static properties as observed in low-energy-electron-diffraction⁷ and x-ray-scattering experiments.⁸ In a previous paper,⁴ we have used the same Hamiltonian to describe the critical dynamics. The results agree very well with the recent inelastic-helium-scattering experiment.² Nevertheless, that study of surface dynamics has been limited to the high-temperature (HT) range, i.e., $T \geq T_c$.

Recent interest in this surface has centered on attempting to describe the surface dynamics at low temperature (LT), where the $c(2 \times 2)$ reconstruction of the W(100) surface lowers the symmetry from C_{4v} to C_{2v} .⁹ Because of lower symmetry, a phonon band gap is expected^{10,11} at the new surface-Brillouin-zone (SBZ) boundary. The vibrational properties for $T \ll T_c$ can be understood within the harmonic picture. However, as the temperature increases towards T_c , the critical fluctuation becomes increasingly important. The band gap will vanish and the vibrational spectrum will evolve continuously into the HT phase described in Ref. 4. The purpose of this paper is to study within the model Hamiltonian approach how the vibrational spectrum evolves from the LT phase into the HT phase, and to identify the interactions in the model Hamiltonian responsible for the occurrence of the band gap at the new SBZ for the LT phase.

In the reconstructed phase, tungsten atoms on a (100) surface form a superlattice structure with two basis atoms whose atomic positions can be written as $\mathbf{x}_i^s = \mathbf{R}_i + \mathbf{s} + u_0 \mathbf{e}^s$. Here i is the cell index, such that $\mathbf{R}_i = a_0(l, m)$, $l + m = \text{even}$, \mathbf{s} is the basis chosen to be (0,0) for the A sublattice and $a_0(1,0)$ for the B sublattice, respectively, u_0 is the amplitude of displacement measured from the (1×1) unreconstructed surface, and \mathbf{e}^s is

its polarization along the (1,1) direction.

We consider a model Hamiltonian ($H = H^{(0)} + H^{(3)}$) of lattice displacements to describe the surface dynamics of W(100). $H^{(0)}$ is the one used in our previous studies^{4,6,12} and can be written in a superlattice form as

$$H^{(0)} = \sum_{i,s} \left[\frac{1}{2M_W} \mathbf{p}_i^s{}^2 + \frac{A}{2} \mathbf{u}_i^s{}^2 + \frac{B}{4} \mathbf{u}_i^s{}^4 + 8H_4 u_{ix}^s{}^2 u_{iy}^s{}^2 \right] + C_1 \sum_{\langle NN \rangle} \mathbf{u}_i^s \cdot \mathbf{u}_j^{s'} + C_2 \sum_{i,s} [u_{ix}^s (u_{jy}^s - u_{ky}^s) + u_{iy}^s (u_{jx}^s - u_{kx}^s)]. \quad (1)$$

Here M_W is the mass of a tungsten atom, and \mathbf{p}_i^s and \mathbf{u}_i^s are the momentum and displacement, respectively, of a tungsten atom of s sublattice on the i th cell. For the on-site terms, A , B , and H_4 are the interaction strengths. For the nearest-neighbor interaction, $C_1 (> 0)$ is the interaction strength and $\langle NN \rangle$ denotes the summation over the nearest neighbors, i.e., $|\mathbf{R}_i + \mathbf{s} - \mathbf{R}_j - \mathbf{s}'| = a_0$. To drive the desired (1×1) to $c(2 \times 2)$ reconstruction upon cooling, $4C_1 - A > 0$ and $B + 8H_4 > 0$ are the minimal conditions in addition to $B > 0$, $H_4 < 0$, and $C_1 > 0$. For the next-nearest-neighbor interaction, C_2 is the interaction strength greater than zero to explain the difference in longitudinal and transverse excitations,^{4,6,8} and the summation is over the next-nearest neighbors, i.e., $\mathbf{R}_i - \mathbf{R}_j = a_0(1, 1)$ and $\mathbf{R}_i - \mathbf{R}_k = a_0(-1, 1)$.

Though $H^{(0)}$ contains dominant features of W(100) reconstruction and surface dynamics, it does not include an interaction related to a surface phonon gap at $T < T_c$. Thus we consider the cubic order neighbor interactions.¹³ Assuming a central force for a pair of nearest neighbors at $\mathbf{R}_i + \mathbf{s}$ and $\mathbf{R}_j + \mathbf{s}'$, we may write the interaction potential as

$$V_{ij}^{ss'} = V(a_0^2 + w_{ij}^{ss'2} + 2\mathbf{R}_{ij}^{ss'} \cdot \mathbf{w}_{ij}^{ss'}) , \quad (2)$$

where $\mathbf{R}_{ij}^{ss'} = \mathbf{R}_i + \mathbf{s} - \mathbf{R}_j - \mathbf{s}'$ with $|\mathbf{R}_{ij}^{ss'}| = a_0$ and $\mathbf{w}_{ij}^{ss'} = \mathbf{u}_i^s - \mathbf{u}_j^{s'}$. Expanding $V_{ij}^{ss'}$ up to the u^3 term, we have

$$V_{ij}^{ss'} \simeq V_0 + V_0^{(1)}(2\mathbf{R}_{ij}^{ss'} \cdot \mathbf{w}_{ij}^{ss'} + \mathbf{w}_{ij}^{ss'2}) + V_0^{(2)}(\mathbf{R}_{ij}^{ss'} \cdot \mathbf{w}_{ij}^{ss'})^2 + 2V_0^{(2)} \mathbf{w}_{ij}^{ss'2} (\mathbf{R}_{ij}^{ss'} \cdot \mathbf{w}_{ij}^{ss'}) + \frac{4}{3} V_0^{(3)} (\mathbf{R}_{ij}^{ss'} \cdot \mathbf{w}_{ij}^{ss'})^3 , \quad (3)$$

where

$$V_0^{(n)} = \frac{\partial^n}{\partial x^n} V(x) \Big|_{x=a_0^2}.$$

The stability of the system requires that the linear term of w should vanish after summation over nearest neighbors, and the harmonic terms were already considered in $H^{(0)}$. Now, the remaining interaction is $H^{(3)}$ of cubic term

$$H^{(3)} = \sum_{\langle NN \rangle} \{ G_1 (\mathbf{u}_i^s - \mathbf{u}_j^{s'})^2 \mathbf{e}_{ij}^{ss'} \cdot (\mathbf{u}_i^s - \mathbf{u}_j^{s'}) + G_2 [\mathbf{e}_{ij}^{ss'} \cdot (\mathbf{u}_i^s - \mathbf{u}_j^{s'})]^3 \}, \quad (4)$$

where G_1 and G_2 are the interaction strengths, the summation is over the nearest neighbors, and $\mathbf{e}_{ij}^{ss'} = (\mathbf{R}_i + \mathbf{s} - \mathbf{R}_j - \mathbf{s}')/a_0$.

The effect of $H^{(3)}$ accounts for the fact that the nearest-neighbor interaction could not be identical for every neighboring pair upon the $c(2 \times 2)$ reconstruction. The distances between the neighboring tungsten atoms are not the same, though the difference ($0.17a_0$ for the ground state) is small enough to be ignored as a first approximation in many previous studies. For the ground state, $H^{(3)}$ gives an interaction energy change $\delta = \pm(G_1 4\sqrt{2} + G_2 2\sqrt{2})u_0^3$ for a pair, where $u_0 = [(4C_1 - A)/(B + 8H_4)]^{1/2}$ is the ground-state amplitude. The (+) sign is for a pair of two surface atoms that get closer after the reconstruction giving repulsive interaction, and the (-) sign is for a pair whose separation increases after reconstruction. Though its contribution to the total energy is zero, $H^{(3)}$ is crucial for the existence of the surface phonon band gap in our model, as shown below. We consider that δ is to be smaller than the harmonic contribution ($C_1 u_0^2$ for a pair), i.e., $|\delta/C_1 u_0^2| = 2\sqrt{2}u_0(2G_1 + G_2)/C_1 < 1$.

First, we consider the quasiharmonic approximation (QHA), which serves as a test of the theory of surface dynamics because it yields the correct behavior in the limit

of $T \ll T_c$, where critical fluctuations are negligible. In this approximation, the tungsten surface atoms are assumed to vibrate harmonically around their average equilibrium positions. Then, we consider a transformation

$$\tilde{u}_{\alpha,i}^s(t) = u_{\alpha,i}^s(t) - \langle u_{\alpha}^s \rangle, \quad (5)$$

where $\tilde{u}_{\alpha,i}^s$ denotes the displacement measured from its equilibrium position $\langle u_{\alpha}^s \rangle = (1/N') \langle \sum_i u_{\alpha,i}^s \rangle$, where $\langle \rangle$ denotes the thermodynamic averages and N' is the number of superlattice unit cells on the W(100) surface. Note that $\langle u_{\alpha}^s \rangle$ is a function of temperature, which vanishes at $T \geq T_c$, and also that $\langle u \rangle \equiv \langle u_x^A \rangle = \langle u_y^A \rangle = -\langle u_x^B \rangle = -\langle u_y^B \rangle$ by symmetry considerations for a single domain structure. Substituting Eq. (5) into the model Hamiltonian, we have the dynamical equation

$$\omega^2(\mathbf{q}) \tilde{u}_{\alpha}^s(\mathbf{q}) = \sum_{s',\beta} D_{\alpha\beta}^{ss'}(\mathbf{q}) \tilde{u}_{\beta}^{s'}(\mathbf{q}) + O(\tilde{u}^2), \quad (6)$$

where $D_{\alpha\beta}^{ss'}(\mathbf{q})$ is the dynamical matrix in the QHA. In Eq. (6), we have used a Fourier transform for a wave vector \mathbf{q} inside of a SBZ defined as

$$\tilde{u}_{\alpha}^s(\mathbf{q}) = \frac{1}{N'} \sum_i \tilde{u}_{\alpha,i}^s e^{-i\mathbf{q} \cdot (\mathbf{R}_i + \mathbf{s})}, \quad (7)$$

where we set $1 \equiv (Ax)$, $2 \equiv (Ay)$, $3 \equiv (Bx)$, $4 \equiv (By)$ in matrix notation.

Surface dynamics on W(100) at finite temperatures cannot be fully described by QHA near the critical region $T \rightarrow T_c$, $\mathbf{q} \rightarrow \mathbf{0}$, where the critical fluctuations are important as well as the anharmonic effects. We examine this effect through the dynamic structure factor $S(\mathbf{q}, \omega) = \int_{-\infty}^{\infty} dt e^{-i\omega t} \langle \tilde{\mathbf{u}}_0(\mathbf{q}, t) \tilde{\mathbf{u}}_0^\dagger(\mathbf{q}) \rangle$, where $\tilde{\mathbf{u}}_0(\mathbf{q}, t) = \mathbf{u}(\mathbf{q}, t) - \langle \mathbf{u}(\mathbf{q}) \rangle$, with $\mathbf{u}(\mathbf{q}) = [u_x^A(\mathbf{q}), u_y^A(\mathbf{q}), u_x^B(\mathbf{q}), u_y^B(\mathbf{q})]^T$. Using Mori's formalism,¹⁴ the Laplace transform of the time-correlation function of lattice fluctuation can be written as a continued fraction:

$$\tilde{S}(\mathbf{q}, z) = \frac{k_B T}{N'} (z + \{ z + \cdots [z + (z + \lambda_n)^{-1} \Delta^{(n)}]^{-1} \cdots \Delta^{(2)} \}^{-1} \Delta^{(1)})^{-1} \chi(\mathbf{q}), \quad (8)$$

where $\chi(\mathbf{q}) = (N'/k_B T) \{ \langle \mathbf{u}(\mathbf{q}) \mathbf{u}^\dagger(\mathbf{q}) \rangle - \langle \mathbf{u}(\mathbf{q}) \rangle \langle \mathbf{u}^\dagger(\mathbf{q}) \rangle \}$ is the static susceptibility tensor by definition and $(\lambda_n)^2 = \Delta^{(n)} + \Delta^{(n-1)}$ using the generalized de Raedt self-consistent prescription.¹⁵ This is related to the dynamical structure factor through the expression $S(\mathbf{q}, \omega) = 2 \text{Re} \tilde{S}(\mathbf{q}, z = i\omega)$. The explicit mathematical expression for expansion parameters $\Delta^{(i)}$ are omitted here but can be easily derived as described in our previous works.^{4,11} They are thermodynamic averages related to the various frequency moments of $S(\mathbf{q}, \omega)$.

To evaluate $\Delta^{(i)}$'s, we have performed standard Monte Carlo (MC) simulation on an $L \times L$ lattice ($L = 20, 60$) with a periodic boundary condition. For simulation, we used dimensionless Hamiltonian parameters, $A = -10$, $B = 40$, $H_4 = -1.85$, $C_1 = 3.75$, $C_2 = 1.875$, $G_1 = 0.1$, and $G_2 = 0.1$. One MC step consisted of two trials per site at

a given temperature. We took 20000 MC steps for thermal averages after the equilibration processes of discarding the initial 5000–10000 MC steps. The starting configuration was always the ground-state one with the orientation of $\langle \underline{u} \rangle$ along (11). We confirmed that our model Hamiltonian gives the desired reconstruction transition of W(100) by monitoring $\langle u \rangle$ and $\chi(\mathbf{q} = 0)$. We identified the apparent transition temperature $T_c = 2.11 \pm 0.03$ for both system sizes using Binder's Monte Carlo renormalization-group method.¹⁶

$S(\mathbf{q}, \omega)$ is then calculated by substituting $\Delta^{(i)}$'s in the continued-fraction expansion. We have obtained qualitatively similar behaviors from the two different approximations for $S(\mathbf{q}, \omega)$ by terminating at the levels of $n = 2$ and 3 of the continued-fraction expansion in Eq. (8). These two approximations result in similar behaviors,

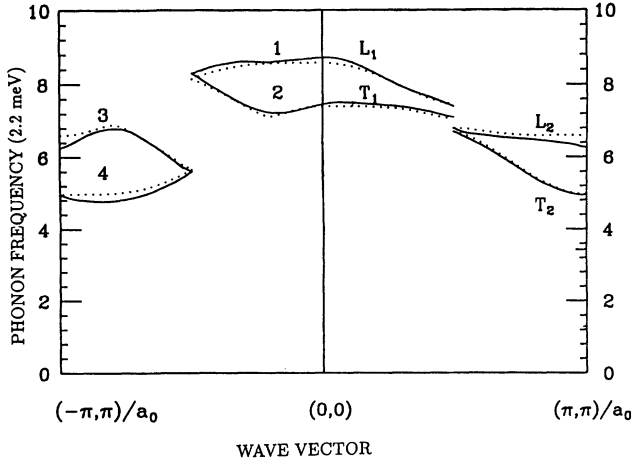


FIG. 1. The surface-phonon-dispersion relations at $T=0.36T_c$ are shown in an extended zone scheme as a function of wave vector. The solid line is from the critical dynamics of the $n=3$ approximation. The dotted line is from the QHA replacing $\langle u \rangle = 0.95u_0/\sqrt{2}$. Input parameters are taken from a 60×60 MC simulation.

though they are slightly different near the transition. We have observed the quantitative convergence between the $n=3$ and $n=4$ approximations in the HT case.⁴ Thus, it is sufficient to use the $n=3$ approximation to represent the results for the current study.

In Fig. 1, we show the phonon dispersion relation for $T=0.36T_c$ from the $n=3$ approximation of $S(\mathbf{q}, \omega)$ using an extended zone scheme. For $\mathbf{q} \parallel [11]$, we have four non-degenerate surface phonon bands whose polarizations are either longitudinal or transverse (labeled L_1 , L_2 , T_1 , and T_2 , respectively). Phonon band gaps exist only for nonzero values of G_1 and G_2 in both longitudinal and transverse branches at $\mathbf{q}_{\parallel} = (\pi, \pi)/2a_0$, which is one of the SBZ boundaries. It is noted that the lowest band is found to be that for the transverse mode for $B + 16H_4 > 0$ in the $T \rightarrow 0$ limit, in contrast to the HT case.⁴ For $\mathbf{q} \parallel [\bar{1}1]$, we also have four surface phonon bands that are not pure longitudinal or transverse modes (labeled 1, 2, 3, and 4). It is clear that the $[11]$ direction is no longer equivalent to the $[\bar{1}1]$ direction below T_c . For this temperature, there is good agreement between the QHA (using $\langle u \rangle = 0.95u_0/\sqrt{2}$ from MC simulation) and $n=3$ critical dynamics. It is noted that the gap at $\mathbf{q}_{\perp} = (\pi, \pi)/2a_0$ reflects the nonzero C_2 , and it should be distinguished from the gap due to G_1 and G_2 terms, which are directly related to the lowering of symmetry by reconstruction.

In Fig. 2(a), we show the dynamic structure factor of longitudinal modes for \mathbf{q}_{\parallel} below and above T_c . It is clear that the band gap opens up for $T < T_c$. In Fig. 2(b), we show the phonon dispersion relation of longitudinal mode, $\omega_{sp} = \omega(\mathbf{q})$ of a wave vector \mathbf{q} along $[11]$ in an extended zone scheme for several temperatures ($T=0, 0.71, 1.43T_c$).¹⁷ At $T=0$, the QHA is used to calculate the dispersion relation. At $T=0.71T_c$, broadening in the phonon spectrum occurs, as does softening. The frequency spectrum of $S(\mathbf{q}, \omega)$ is so broad that it is somewhat difficult to distinguish the phonon frequency from the

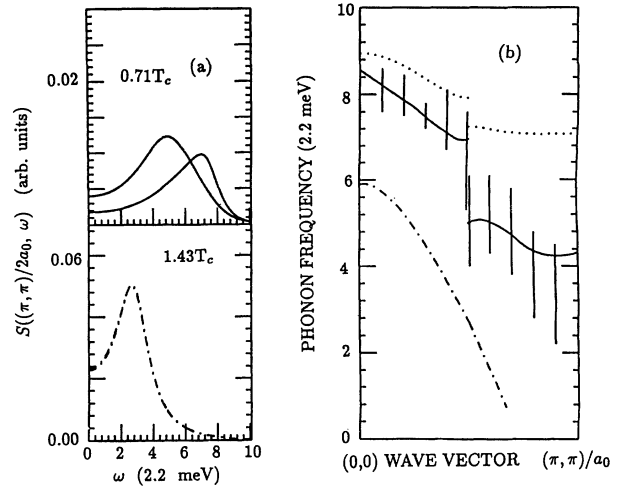


FIG. 2. (a) The dynamic structure factor of longitudinal mode at $\mathbf{q} = (\pi, \pi)/2a_0$ is shown as a function of frequency for temperatures below and above transition. (b) The surface-phonon-dispersion relation of longitudinal excitation for $\mathbf{q} \parallel [11]$ is shown in an extended zone scheme for $T=0$ (dotted lines), $T=0.71T_c$ (solid lines), and $T=1.43T_c$ (dotted-dashed lines) using the critical dynamics of the $n=3$ approximation. The vertical line for the data of $T=0.71T_c$ shows the characteristic width. Input parameters are taken from a 60×60 MC simulation.

peak of $S(\mathbf{q}, \omega)$. For that reason, we also show the characteristic width in the figure. It is noted that the QHA, which predicts a sharp phonon peak, fails at temperature $T=0.71T_c$, even though $\langle u \rangle$ is still large (about $0.84u_0/\sqrt{2}$). This implies that the phonon properties at $T \ll T_c$ are very different from that just below T_c even when $c(2 \times 2)$ order is already well developed. At $T=1.43T_c$, above the transition, the two longitudinal modes at \mathbf{q}_{\parallel} are degenerate without a gap, as expected, when the order parameter vanishes.

Our model does not include the vertical motion. Also, the surface mode of long wavelength tends to penetrate into the bulk. The use of a purely two-dimensional model does not give a good description of surface dynamics for $\mathbf{q} \rightarrow 0$, for which $\omega(\mathbf{q}) \rightarrow 0$. For this reason, only the results for large wave vectors can be compared with the experimental data. So far, the available data are very limited, and we could not draw a definite conclusion. Further experimental studies, such as those of the detailed temperature dependence of phonon dispersion and the detection of transverse modes,¹⁸ will be fruitful for understanding the static and dynamic properties of $W(100)$.

In summary, we have extended the study of the critical dynamics of $W(100)$ to the regime $T < T_c$ using a simple model Hamiltonian and a recently developed method of critical dynamics. We demonstrate that a surface phonon gap will open at the new SBZ boundary of the reconstructed $W(100)$ surface below T_c , and identify the interactions in the model Hamiltonian responsible for this behavior. Strong temperature dependences of surface phonon excitations are observed, which are due to the strong anharmonicity and the critical fluctuations.

This work was supported in part by an ONR contract.

*Present address: Department of Physics, Hong-Ik University, 72-1, Sangsu-Dong, Mapo-Gu, Seoul, 121-791, Korea.

¹J. P. Woods and J. L. Erskine, *Phys. Rev. Lett.* **55**, 2595 (1985); *J. Vac. Sci. Technol. A* **4**, 1414 (1986).

²H.-J. Ernst, E. Hulpke, and J. P. Toennies, *Phys. Rev. Lett.* **58**, 1941 (1987).

³C. Z. Wang, A. Fasolino, and E. Tosatti, *Phys. Rev. Lett.* **59**, 1845 (1987); *Phys. Rev. B* **37**, 2116 (1988); *Europhys. Lett.* **7**, 263 (1988).

⁴W. K. Han, S. C. Ying, and D. Sahu, *Phys. Rev. B* **41**, 4403 (1990).

⁵T. E. Felner, R. A. Barker, and P. J. Estrup, *Phys. Rev. Lett.* **38**, 1138 (1977); M. K. Debe and D. A. King, *ibid.* **39**, 708 (1977).

⁶W. K. Han and S. C. Ying, *Phys. Rev. B* **41**, 9163 (1990).

⁷J. F. Wendelken and G. C. Wang, *Phys. Rev. B* **32**, 7542 (1985).

⁸I. K. Robinson, A. A. MacDowell, M. S. Altman, P. J. Estrup,

K. Evans-Lutterodt, J. D. Brock, and R. J. Birgeneau, *Phys. Rev. Lett.* **62**, 1294 (1989).

⁹D. A. King, *Phys. Scr. T* **4**, 34 (1981).

¹⁰H.-J. Ernst, Ph.D. thesis, 1988.

¹¹T. Reinecke and S. C. Ying, *Phys. Rev. B* **43**, 12 234 (1991).

¹²Similar model Hamiltonians have been used to study W(100) by L. D. Roelofs and J. F. Wendelken, *Phys. Rev. B* **34**, 3319 (1986).

¹³W. K. Han, Ph.D. thesis, 1991.

¹⁴H. Mori, *Prog. Theor. Phys.* **34**, 399 (1965).

¹⁵H. De Raedt, *Phys. Rev. B* **19**, 2585 (1979).

¹⁶K. Binder, *Phys. Rev. Lett.* **47**, 693 (1981).

¹⁷The $T=0$ result here is meant to represent the $T \ll T_c$ region. Quantum effects are neglected here.

¹⁸E. J. Jeong and J. L. Erskine, *Bull. Am. Phys. Soc.* **34**, 947 (1989); H. Ibach (private communication).